2nd National Congress
" on the development of agricultural scienceand natural resources "
GORGAN , 11 , May , 2016

An underrelaxed-modified Picard iteration scheme for simulation of 3D wetting pattern under drip irrigation using Richards' equation on non-orthogonal grids

Mohammadreza Naghedifar
Department of Water Engineering, College of Agriculture, Ferdowsi University of Mashhad (FUM), Mashhad, Iran
m.rezanaghedifar@stu.um.ac.ir

Hossein Ansari [1]
Department of Water Engineering, College of Agriculture, Ferdowsi University of Mashhad (FUM), Mashhad, Iran
Ansary@um.ac.ir

Sayyed Majid Hasheminia
Department of Water Engineering, College of Agriculture, Ferdowsi University of Mashhad (FUM), Mashhad, Iran
hasheminia@um.ac.ir

Ali Naghi Ziaei
Department of Water Engineering, College of Agriculture, Ferdowsi University of Mashhad (FUM), Mashhad, Iran
an-ziaei@um.ac.ir

Abstract
The knowledge of soil wetting pattern dimensions is one of the most important design parameters in drip irrigation systems. In this study, a three dimensional (3D) FORTRAN code based on finite volume approach is provided to investigate about wetting pattern characteristics under line source and point source drip irrigation systems. The coordinate transformation method is used to transform the governing equation from physical space to computational space. The model was validated with data obtained by HYDRUS 2D software. The results showed that the model is able to predict soil wetting pattern under both line source (2D model) and point source (3D model) irrigation systems in different soil textures. Eventually, the ability of this model for simulation of soil water redistribution process was investigated and acceptable results were obtained.

Keywords: Numerical model, Subsurface flow, Finite volume, trickle irrigation, Coordinate transformation

Introduction
Increasing water demand of irrigated fields due to worldwide population growth and limited water resources necessitates irrigation water management, which is known to be the largest source of water withdrawal in most regions [1]. The use of micro-irrigation systems has been accepted and developed rapidly during past decades [2, 3]. The main advantage of micro-irrigation systems is water use efficiency improvement and higher crop yield enhancement [3, 4]. Drip irrigation is one of the most well-known and widely used irrigation systems due to its flexibility and multitasking i.e. it enables farmers to apply water and fertilizer simultaneously [5]. The efficiency of drip irrigation systems mainly relies on the performance of emitters. Emitter spacing, depth of lateral placement below soil surface and system pressure for delivering required amount of water to the plant, which are crucial parameters in design and management of drip irrigation systems, are directly influenced by dimensions of soil wetting patterns [6].
A number of methods are proposed for determination of soil wetting pattern [7] such as semi-empirical equations [8], analytical approaches [9, 10] and numerical methods [11-14]. Among the aforementioned methodologies, numerical methods are the most complicated yet precise and comprehensive method for general situations. Available models such as HYDRUS 2D/3D [15] and Drip-Irriwater [16] numerically solve 2D or 3D Richards' equation.
Richards' equation is commonly formulated in three forms; water content based, pressure head based and mixed form [17, 18]. Pressure head based Richards' equation usually leads to incorrect predictions of head pressure distribution. This fact stems from relatively large mass balance errors which occurs in numerical solution [19, 20]. On the other hand, water content based Richards' equation do not show an appropriate results for heterogeneous soils. Because the driving force for water movement is not the water content gradient, but the pressure head gradient [19]. Ceila (1990) proposed a mass conservative scheme, known as modified Picard scheme, for mixed form Richards' equation that solves with perfect mass balance and prevents drawbacks of the other two approaches.
Highly nonlinearity inherent in Richards' equation makes it necessary to be linearized. Paniconi and Putti (1994)[21] made a comparison of two widely used procedures for solving nonlinear equations i.e. Picard and Newton-Raphson. They stated that Picard iteration procedure is an appropriate and simple method for a large range of numerical problems. However, it may fail to converge in some cases. On the other hand, while Newton-Raphson approach is second-order accurate and,

1-Corresponding Author

thus, converges faster, it is sensitive to initial guess. In this paper a modified-under relaxation Picard procedure is used to linearize Richards' equation [20, 22] and a three dimensional FORTRAN code using finite volume approach is provided to solve the mixed form of Richards' equation on non-orthogonal grids.

Methods and materials

Governing equation

The governing equation for 3D saturated-unsaturated water flow in porous media is Richards' equation [23]. In this study, the mixed form of Richards' equation is adopted, assuming negligible hysteresis effect [18].

$$\frac{\partial \theta}{\partial t} - \nabla.\left(K_{unsat}\,\nabla(\psi + Z)\right) - q_{sub} = 0 \qquad (1)$$

Where θ, h, K, t, z denote volumetric water content ($L^3.L^{-3}$), soil water pressure head (L), unsaturated hydraulic conductivity ($L.T^{-1}$), time (T) and vertical space coordinate (L), respectively. q_{sub} represents the source/sink term. The soil water content-pressure head curve $\theta(h)$ and unsaturated hydraulic conductivity K are described using Van Genuchten [24] and Mualem's [25] models as follows:

$$\theta(h) = \begin{cases} \theta_r + \dfrac{\theta_s - \theta_r}{(1 + (\alpha\,\psi)^n)^m} & , \ \psi < 0 \\ \theta_s & , \ \psi \geq 0 \end{cases} \qquad (2)$$

$$K(h) = \begin{cases} K_s S_e^{\frac{1}{2}} \left(1 - \left(1 - S_e^{\frac{1}{m}}\right)^m\right)^2 & , \ \psi < 0 \\ K_s & , \ \psi \geq 0 \end{cases} \qquad (3)$$

$$S_e = \frac{\theta - \theta_r}{\theta_s - \theta_r} \qquad (4)$$

Where S_e is effective saturation ($L^3.L^{-3}$), θ_s and θ_r are saturated and residual water contents ($L^3.L^{-3}$), $\alpha\ (L^{-1}), m = 1 - \frac{1}{n}$, and n are empirical fitting parameters whose values depend on the soil properties, K_s is the saturated hydraulic conductivity ($L.T^{-1}$). The constant parameters of Van Genuchten-Mualem's model were estimated using ROSETTA [26] and RETC [27, 28] codes. ROSETTA is a well-known neural network based software used for estimating soil hydraulic parameters [26]. The RETC program iteratively fits a number of analytical functions to find the optimum values of Van Genuchten parameters using least squares objective function [29]. Parameters of Van Genuchten-Mualem equations used in this study are listed in "Table 1".

Table 1- Parameters of Van Genuchten's model

Soil type	θ_s	θ_r	$\alpha\ (\frac{1}{cm})$	n	$K_s\ (\frac{cm}{hr})$
Clay	0.38	0.068	0.008	1.09	4.8
Loam	0.43	0.078	0.036	1.56	24.96
Sand	0.43	0.045	2.68	0.145	712.8

Spatial Discretization

In this study, finite volume scheme is used to discretize 3D Richards' equation. Non-orthogonal control volumes resulted from integrating equation 1 as follows:

$$\int_{Vol} \frac{\partial \theta}{\partial t}\, dVol - \int_A K\,\vec{\nabla}(\psi + z).\vec{\boldsymbol{n}}\, dA - \int_{Vol} (q_{sub})\, dVol = 0 \qquad (5)$$

Where Vol and A represent volume and boundary of an arbitrary control volume. $\vec{\boldsymbol{n}}$ is normal vector to control volume boundary. θ and ψ are assumed to be the cell-averaged values from the finite volume approximation. Therefore, using Gauss-Green divergence theorem, equation 5 can be written as:

$$\begin{aligned} Vol_{i,j,k}\,\frac{\partial \theta_{i,j,k}}{\partial t} - \Bigg[\sum_b K_b \Bigg(& \frac{\partial(\psi + z)}{\partial x}\,\vec{\imath} \\ & + \frac{\partial(\psi + z)}{\partial y}\,\vec{\jmath} \\ & + \frac{\partial(\psi + z)}{\partial z}\,\vec{k} \Bigg).\left(A_x\vec{\imath} + A_y\,\vec{\jmath} + A_z\vec{k}\right) \Bigg]_{i,j,k} \\ & - Vol_{i,j,k}\left(q_{sub} + q_{e,sub}\right)_{i,j,k} \\ & = 0 \end{aligned} \qquad (6)$$

Where $b = \{w, e, s, n, bot, top\} = \left\{\begin{matrix} \left(i - \frac{1}{2}, j, k\right), \left(i + \frac{1}{2}, j, k\right), \left(i, j - \frac{1}{2}, k\right), \\ \left(i, j + \frac{1}{2}, k\right), \left(i, j, k + \frac{1}{2}\right), \left(i.j, k - \frac{1}{2}\right) \end{matrix}\right\}$ denotes x, y and z directions. $i + \frac{1}{2}$ and $i - \frac{1}{2}$ show the control volume interfaces. To calculate unsaturated hydraulic conductivity at the cell-interface, arithmetic average of unsaturated hydraulic conductivity in surrounding cell centers along each direction is used which has been recommended by researchers [30, 31]. The averaged unsaturated hydraulic conductivity at $(\mathrm{i}, \mathrm{j}, \mathrm{k} + \frac{1}{2})$ is calculated as follows:

$$k_{i,j,k+\frac{1}{2}} = \frac{k_{i,j,k} + k_{i,j,k+1}}{2} \tag{7}$$

Coordinate Transformation on nonorthogonal grids

In this study, we have used coordinate transformation method which is based on tensor analysis and has been widely used in Computational Fluid Dynamics (CFD) [32]. Using this method, governing equation is transformed from physical space $(x_1, x_2, x_3) = (x, y, z)$ to computational space $(\xi_1, \xi_2, \xi_3) = (\xi, \eta, \zeta)$ ("Figure 1").

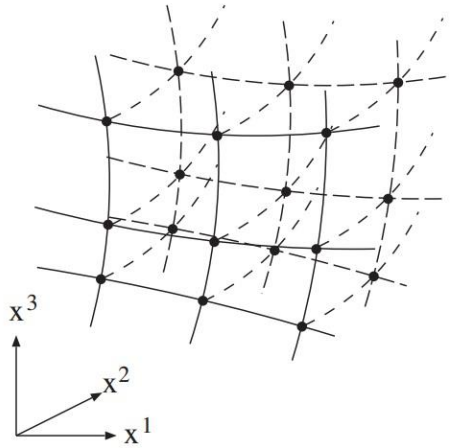

(a)

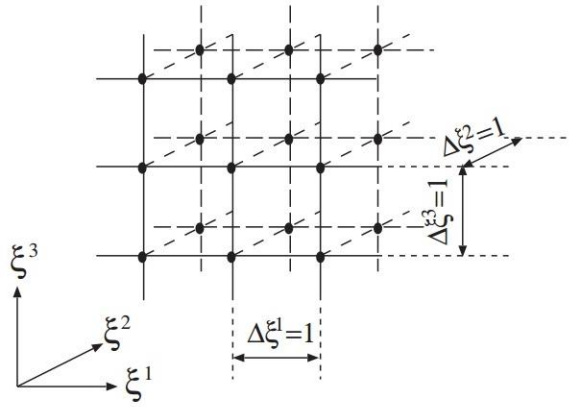

(b)

Figure 1 – Illustration of (a) Physical space and (b) Computational space in coordinate transformation method

To transform gradients of $(\psi + z)$, chain rule is used.

$$\frac{\partial(\psi+z)}{\partial x_i} = \frac{\partial(\psi+z)}{\partial \xi}.\xi_{x_i} + \frac{\partial(\psi+z)}{\partial \eta}.\eta_{x_i} + \frac{\partial(\psi+z)}{\partial \zeta}.\zeta_{x_i} \tag{8}$$

Where $i = \{x, y, z\}$. Transformation metrics are claculated as follows,

$$\begin{aligned}
\xi_x &= \frac{(y_\eta\, z_\zeta - y_\zeta\, z_\eta)}{J} \\
\xi_y &= \frac{(z_\eta\, x_\zeta - z_\zeta\, x_\eta)}{J} \\
\xi_z &= \frac{(x_\eta\, y_\zeta - x_\zeta\, y_\eta)}{J} \\
\eta_x &= \frac{(y_\zeta\, z_\xi - y_\xi\, z_\zeta)}{J} \\
\eta_y &= \frac{(z_\zeta\, x_\xi - z_\xi\, x_\zeta)}{J} \\
\eta_z &= \frac{(x_\zeta\, y_\xi - x_\xi\, y_\zeta)}{J} \\
\zeta_x &= \frac{(y_\xi\, z_\eta - y_\eta\, z_\xi)}{J} \\
\zeta_y &= \frac{(z_\xi\, x_\eta - z_\eta\, x_\xi)}{J} \\
\zeta_z &= \frac{(x_\xi\, y_\eta - x_\eta\, y_\xi)}{J}
\end{aligned} \tag{9}$$

Where J is the Jacobian of transformation which is calculated as follows,

$$J = x_\xi\,(y_\eta\, z_\zeta - y_\zeta\, z_\eta) + x_\eta(y_\zeta\, z_\xi - y_\xi\, z_\zeta) + x_\zeta(y_\xi\, z_\eta - y_\eta\, z_\xi) \tag{10}$$

Combining equations 6, 8, 9, 10 transformed form of three dimensional Richards' equation is as follows,

$$Vol_{i,j,k}\,\frac{\partial \theta_{i,j,k}}{\partial t} - \left[\sum_b K_b \left(Coef_\xi \frac{\partial(\psi+z)}{\partial \xi} + Coef_\eta \frac{\partial(\psi+z)}{\partial \eta} + Coef_\zeta \frac{\partial(\psi+z)}{\partial \zeta}\right)_b\right]_{i,j,k} - Vol_{i,j,k}\,(q_{sub})_{i,j,k} = 0 \tag{11}$$

In which,

$$\begin{aligned} Coef_{\xi} &= \xi_x . A_x + \xi_y . A_y + \xi_z . A_z \\ Coef_{\eta} &= \eta_x . A_x + \eta_y . A_y + \eta_z . A_z \\ Coef_{\zeta} &= \zeta_x . A_x + \zeta_y . A_y + \zeta_z . A_z \end{aligned} \quad (12)$$

The transformed grid is orthogonal and its mesh size is typically set to 1 ("Figure 1"). Therefore, the gradients of $(\psi + z)$ can be discretized using a finite difference approach. For example, the value at $(\mathrm{i}, \mathrm{j}, \mathrm{k} + \frac{1}{2})$ is given by following set of equations,

$$\begin{aligned} &\left.\frac{\partial(\psi+z)}{\partial\xi}\right|_{i,j,k+\frac{1}{2}} \\ &= \frac{1}{2}\left[\frac{(\psi+z)_{i+1,j,k} - (\psi+z)_{i-1,j,k}}{2\,\Delta\xi}\right. \\ &\left. + \frac{(\psi+z)_{i+1,j,k+1} - (\psi+z)_{i-1,j,k+1}}{2\,\Delta\xi}\right], \\ &\left.\frac{\partial(\psi+z)}{\partial\eta}\right|_{i,j,k+\frac{1}{2}} \\ &= \frac{1}{2}\left[\frac{(\psi+z)_{i,j+1,k} - (\psi+z)_{i,j-1,k}}{2\,\Delta\eta}\right. \\ &\left. + \frac{(\psi+z)_{i,j+1,k+1} - (\psi+z)_{i,j-1,k+1}}{2\,\Delta\eta}\right], \\ &\left.\frac{\partial(\psi+z)}{\partial\zeta}\right|_{i,j,k+\frac{1}{2}} \\ &= \frac{(\psi+z)_{i,j,k+1} - (\psi+z)_{i,j,k}}{\Delta\zeta} \end{aligned} \quad (13)$$

And the gradients of $\frac{\partial x_i}{\partial \xi_j}$ are approximated in the same manner, as

$$\begin{aligned} \left.\frac{\partial x_i}{\partial\xi}\right|_{i,j,k+\frac{1}{2}} &= \frac{1}{2}\left[\frac{x_{i+1,j,k} - x_{i-1,j,k}}{2\,\Delta\xi}\right. \\ &\left. + \frac{x_{i+1,j,k+1} - x_{i-1,j,k+1}}{2\,\Delta\xi}\right] \\ \left.\frac{\partial x_i}{\partial\eta}\right|_{i,j,k+\frac{1}{2}} &= \frac{1}{2}\left[\frac{x_{i,j+1,k} - x_{i,j-1,k}}{2\,\Delta\eta}\right. \\ &\left. + \frac{x_{i,j+1,k+1} - x_{i,j-1,k+1}}{2\,\Delta\eta}\right] \\ \left.\frac{\partial x_i}{\partial\zeta}\right|_{i,j,k+\frac{1}{2}} &= \frac{x_{i,j,k+1} - x_{i,j,k}}{\Delta\zeta} \end{aligned} \quad (13)$$

Temporal Discretization and linearization

Equation 1 is a second-order highly-nonlinear partial differential equation that necessitates linearization and requires the knowledge of initial and boundary conditions. In this study underrelaxation-modified Picard iteration is used to linearize and to achieve an excellent mass balance in mixed form Richards' equation [20, 22].

A backward Euler method is used for temporal discretization of equation 6. To avoid large mass balance error, we have used the technique presented by Ceila et al. (1990) {Celia, 1990 #13}. Using their approach, which is based on Taylor series expansion, the unsteady term of equation (1) is rewritten as,

$$\begin{aligned} \frac{\theta_{i,j,k}^{n+1,m+1} - \theta_{i,j,k}^{n}}{\Delta t} &= \frac{\theta_{i,j,k}^{n+1,m} - \theta_{i,j,k}^{n}}{\Delta t} \\ &+ \frac{C_{w\,i,j,k}^{\,n+1,m} \cdot \left(\psi_{i,j,k}^{n+1,m+1} - \psi_{i,j,k}^{n+1,m}\right)}{\Delta t} \end{aligned} \quad (14)$$

Using Picard iteration, equation (11) is eventually linearized as,

$$\begin{aligned} &Vol_{i,j,k}\left[\frac{\theta_{i,j,k}^{n+1,m} - \theta_{i,j,k}^{n}}{\Delta t}\right. \\ &\left. + \frac{C_{w\,i,j,k}^{\,n+1,m} \cdot \left(\psi_{i,j,k}^{n+1,m+1} - \psi_{i,j,k}^{n+1,m}\right)}{\Delta t}\right] - \left\{\sum_b K_b^{n+1}\right. \\ &+ Coef_{\eta}\left(\frac{\partial(\psi+z)}{\partial\eta}\right)^{n+1,m+1} \\ &\left. + Coef_{\zeta}\left(\frac{\partial(\psi+z)}{\partial\zeta}\right)^{n+1,m+1}\right]_b\Bigg\}_{i,j,k} \\ &- Vol_{i,j,k}\,(q_{sub})_{i,j,k}^{n+1,m} = 0 \end{aligned} \quad (15)$$

Where n and m represent time step and number of iterations, respectively. The robusstness and convergence rate is enhanced using an underrelaxation approach is used,

$$\begin{aligned} \psi_{i,j,k}^{n+1,m+1} &= \psi_{i,j,k}^{n+1,m} \\ &+ \varphi_{sub}\left(\psi_{i,j,k}^{n+1,m+1} - \psi_{i,j,k}^{n+1,m}\right) \end{aligned} \quad (14)$$

Where, φ_{sub} is the relaxation factor. Linear system of equations is solved using Alternating Direction Implicit (ADI) method.

Results and discussion

1D infiltration problem

The presented model was first verified using a 1D infiltration condition in fine, medium and coarse-textured soils ("Table 1"). The upper and lower boundaries were set as $\psi_{upper} = -0.2$ m and $\psi_{lower} = -10$ m. The other four boundaries were set as no-flow boundary condition and duration of simulation was 12 hours. "Figure 2" shows the dimensions of the soil block in which infiltration occurs.

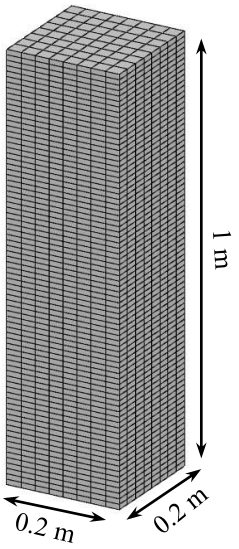

Figure 2- Dimensions of
1D - infiltration test case.

Four orthogonal grids were tested in this study i.e. $(9 \times 9 \times 21)$, $(9 \times 9 \times 41)$, $(9 \times 9 \times 81)$, $(9 \times 9 \times 161)$ and $(9 \times 9 \times 321)$. To study mesh independency of model, the mesh size was refined in z direction. "Figure 7" and "Figure 5" show the comparison between the results obtained by the presented model and HYDRUS-simulated results. It shows that mesh refinement results in convergence to HYDRUS-1D simulations.

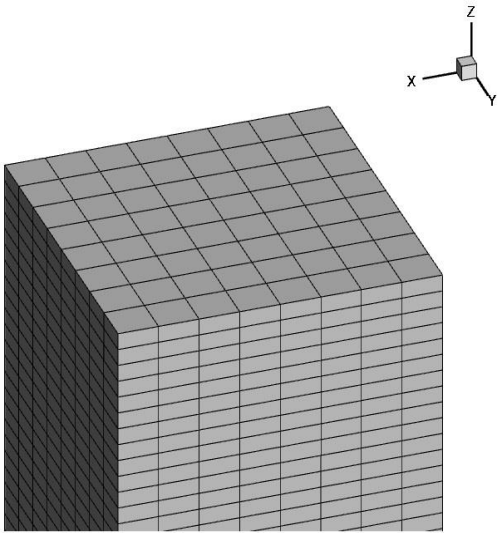

(a)

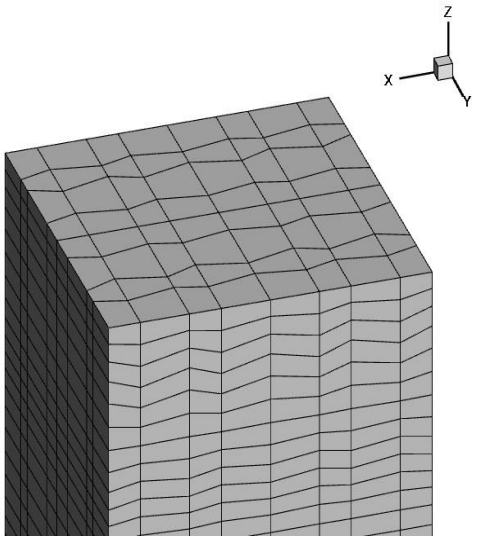

(b)

Figure 3- Illustration of (a) orthogonal and (b) non-orthogonal infiltration test case.

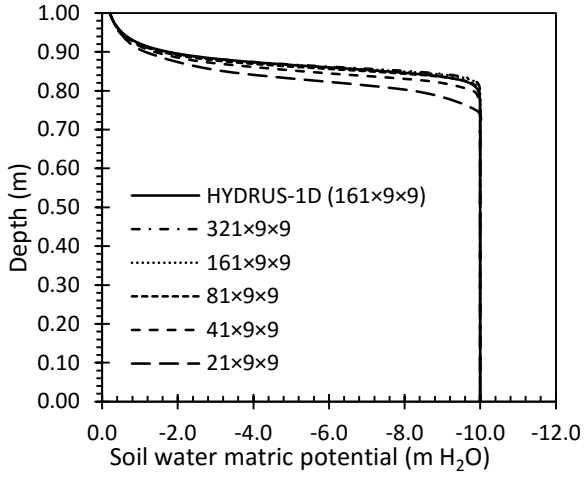

(a)

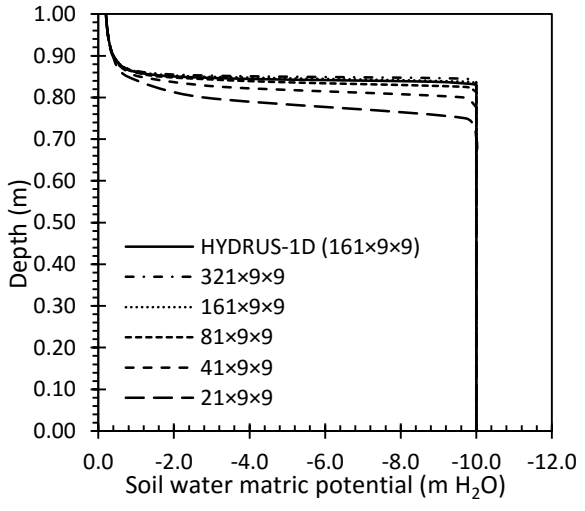

(b)

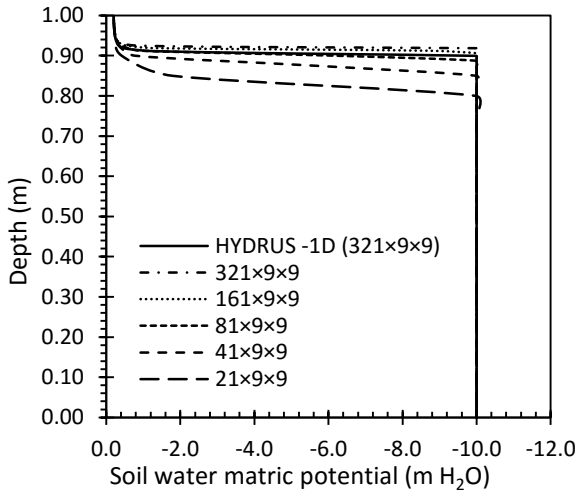

(c)

Figure 4- Illustration of (a) Clay, (b) Loam and (c) Sandy soil on orthogonal grids for infiltration test case.

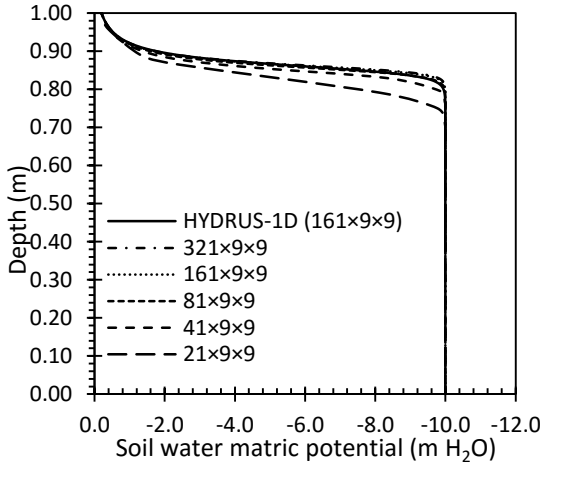

(a)

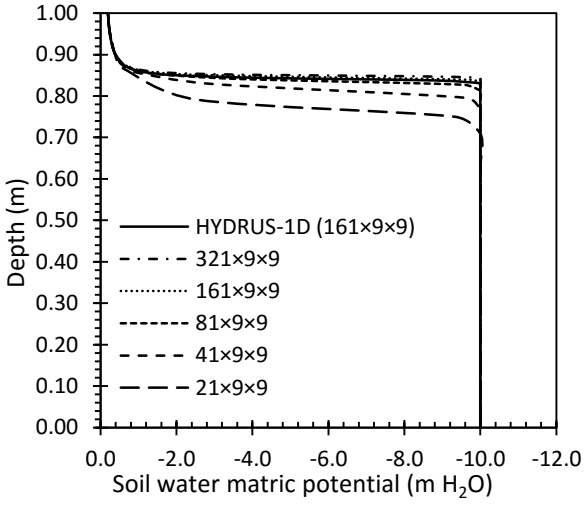

(b)

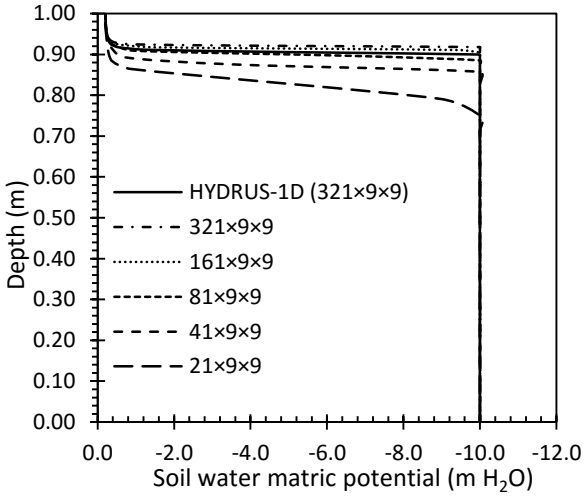

(c)

Figure 5- Illustration of (a) Clay, (b) Loam and (c) Sandy soil on non-orthogonal grids for infiltration test case.

Estimation of a 2D wetting pattern of a line source drip irrigation

Thereafter, the presented model was used to simulate a 2D soil wetting pattern under line source drip irrigation. The same boundary values were set at boundaries. However, the top boundary was set as no flow boundary except for nodal values at line source which were set as $\psi = -0.1\ m$ ("Figure 6"). The results were compared with HYDRUS 2D simulations and are shown in "Figure 1". Good agreement is observed between water content isolines obtained by both models. The homogenous nature of soil led to a symmetric wetting pattern. Using Figure 1, we could simply estimate lateral spacing in drip irrigation design. In this case, the radius of semicircle-shaped soil wetting pattern is about 15 cm. This procedure could be followed for dual-drip irrigation to investigate lateral spacing considering the overlapped wetted pattern.

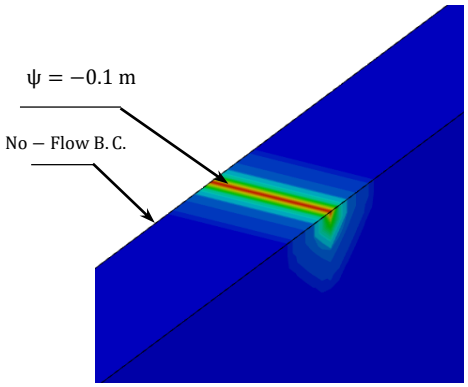

Figure 6 – Comparison of HYDRUS simulation of 2D infiltration pattern in a loamy soil with those obtained by presented model after 12 hours.

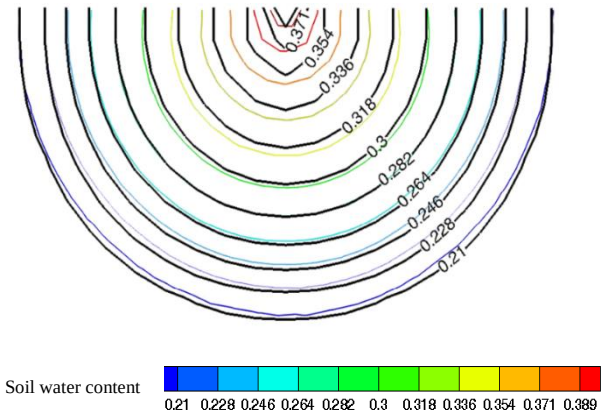

Figure 7 – Comparison of HYDRUS simulation (colorful isolines) of 2D infiltration pattern within loamy soil with those obtained by presented model (solid dark lines) after 12 hours.

Three dimensional soil wetting pattern of a point source drip irrigation

A three-dimensional test case was provided to simulate soil wetting pattern resulting from a point source drip irrigation in a silty soil. The soil characteristics are shown in "Table 1". Irrigation lasted two hours and redistribution process monitored for 12 hours. Western, eastern, northern and southern walls were set as no-flow boundary conditions. Dirichlet boundary condition was set at lower boundary condition whose amount equaled initial values i.e. $\psi = -2.0$ m . Upper boundary was set as Constant-flow boundary condition (Neumann type) during irrigation. The constant recharge flow which was applied as a point source equaled $5.55 \times 10^{-7}\ \frac{m^3}{s}\ (2\frac{\text{lit}}{\text{hr}})$ that infiltrated into the soil through a cell with about 3.5 cm^2 surface area.

$$q = -k_{sat}\nabla(\psi + z).dA \qquad (15)$$

Where q is water flux (L/T), k_{sat} is saturated hydraulic conductivity (L/T) and ψ is soil pressure head, respectively. After two hours, upper boundary condition switches to no-flow boundary condition for all nodal values. "Figure 8" shows the structure and dimension of 3D point source drip irrigation.

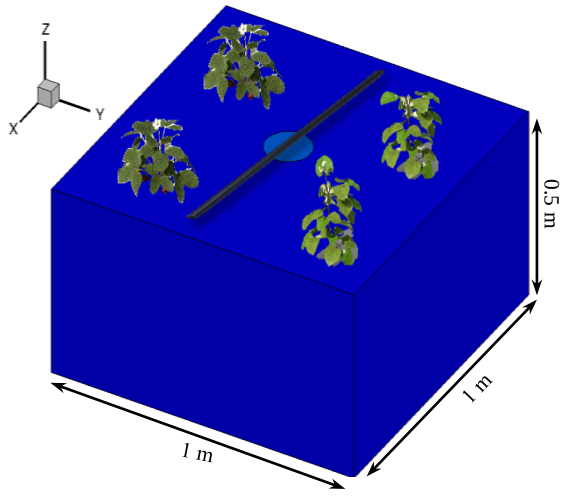

Figure 8 – Structure and dimensions of 3D irrigation/redistribution process simulation.

"Figure 9" illustrates the surface/subsurface wetting pattern at the end of simulated redistribution process. Water flow within homogenous soil which is governed by diffusion process, led to an axisymmetric soil wetting pattern. In this case soil wetting pattern has a depth of 27.5 cm and surface width of 18.75 cm.

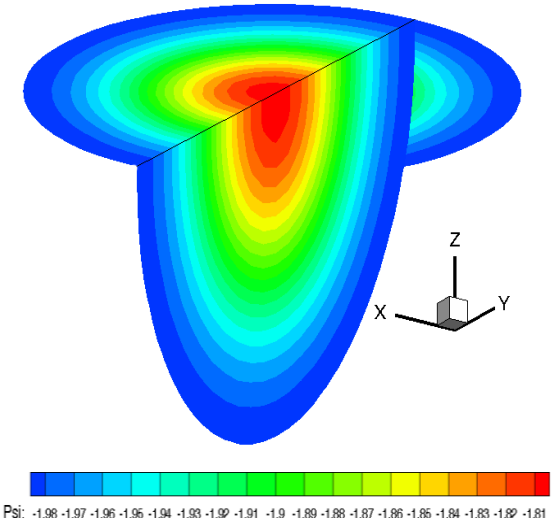

Figure 9 – Surface and subsurface wetting pattern at the end of simulated redistribution process.

Conclusions

A 3D finite volume FORTRAN code using coordinate transformation method was developed for a line source and point source drip irrigation. This model could alleviate drip irrigation design with different boundary conditions and soil types. The infiltration process within fine, medium and coarse-textured soils were simulated and results were compared with those obtained by HYDRUS-1D software. Redistribution process in three dimensions was modeled. It was shown that wetting pattern was acceptably simulated by the proposed model. This 3D illustration could profoundly help drip irrigation system experts, designers and managers.

Reference

1. Spelman, D., K.-D. Kinzli, and T. Kunberger, *Calibration of the 10HS Soil Moisture Sensor for Southwest Florida Agricultural Soils.* Journal of Irrigation and Drainage Engineering, 2013. **139**(12): p. 965-971.
2. Ayars, J., et al., *Subsurface drip irrigation of row crops: a review of 15 years of research at the Water Management Research Laboratory.* Agricultural water management, 1999. **42**(1): p. 1-27.
3. Elmaloglou, S., E. Diamantopoulos, and N. Dercas, *Comparing soil moisture under trickle irrigation modeled as a point and line source.* Agricultural water management, 2010. **97**(3): p. 426-432.
4. Batchelor, C., C. Lovell, and M. Murata, *Simple microirrigation techniques for improving irrigation efficiency on vegetable gardens.* Agricultural Water Management, 1996. **32**(1): p. 37-48.
5. Malek, K. and R.T. Peters, *Wetting pattern models for drip irrigation: new empirical model.* Journal of Irrigation and Drainage Engineering, 2010. **137**(8): p. 530-536.
6. Singh, D., et al., *Simulation of soil wetting pattern with subsurface drip irrigation from line source.* Agricultural water management, 2006. **83**(1): p. 130-134.
7. Subbaiah, R., *A review of models for predicting soil water dynamics during trickle irrigation.* Irrigation Science, 2013. **31**(3): p. 225-258.
8. Schwartzman, M. and B. Zur, *Emitter spacing and geometry of wetted soil volume.* Journal of Irrigation and Drainage Engineering, 1986. **112**(3): p. 242-253.
9. Chen, J.M., Tan, Y. C., Chen, Y. Z. W., *A study of the infiltration of trickle irrigation*, in *7th Int. Micro Irrigation Congress*. 2006: Kuala Lumpur, Malaysia.
10. Philip, J.R., *Travel times from buried and surface infiltration points sources.* Water resources research, 1984(20): p. 990–994.
11. Naglič, B., et al., *Numerical investigation of the influence of texture, surface drip emitter discharge rate and initial soil moisture condition on wetting pattern size.* Irrigation Science, 2014. **32**(6): p. 421-436.
12. Skaggs, T., et al., *Comparison of HYDRUS-2D simulations of drip irrigation with experimental observations.* Journal of irrigation and drainage engineering, 2004. **130**(4): p. 304-310.
13. Cook, F., et al., *Modelling trickle irrigation: comparison of analytical and numerical models for estimation of wetting front position with time.* Environmental Modelling & Software, 2006. **21**(9): p. 1353-1359.
14. Cote, C.M., et al., *Analysis of soil wetting and solute transport in subsurface trickle irrigation.* Irrigation Science, 2003. **22**(3-4): p. 143-156.
15. Ŝimùnek, J., M. Ŝejna, and M.T. van Genuchten, *The HYDRUS Software Package for Simulating Two-and Three-Dimensional Movement of Water, Heat, and Multiple Solutes in Variably-Saturated Media, Technical Manual (Version 1.0).* PC-progress. Prague, Czech Republic, 2006: p. 241.
16. Arbat, G., et al., *Drip-Irriwater: Computer software to simulate soil wetting patterns under surface drip irrigation.* Computers and electronics in agriculture, 2013. **98**: p. 183-192.
17. Kavetski, D., P. Binning, and S. Sloan, *Adaptive time stepping and error control in a mass conservative numerical solution of the mixed form of Richards equation.* Advances in water resources, 2001. **24**(6): p. 595-605.
18. Jury, W.A. and R. Horton, *Soil physics*. 2004: John Wiley & Sons.
19. Šimůnek, J., *Models of water flow and solute transport in the unsaturated zone.* Encyclopedia of hydrological sciences, 2005.

20. Celia, M.A., E.T. Bouloutas, and R.L. Zarba, *A general mass-conservative numerical solution for the unsaturated flow equation.* Water resources research, 1990. **26**(7): p. 1483-1496.
21. Paniconi, C. and M. Putti, *A comparison of Picard and Newton iteration in the numerical solution of multidimensional variably saturated flow problems.* Water Resources Research, 1994. **30**(12): p. 3357-3374.
22. Durbin, T. and D. Delemos, *Adaptive underrelaxation of Picard iterations in ground water models.* Groundwater, 2007. **45**(5): p. 648-651.
23. Richards, L.A., *Capillary conduction of liquids through porous mediums.* Journal of Applied Physics, 1931. **1**(5): p. 318-333.
24. Van Genuchten, M.T., *A closed-form equation for predicting the hydraulic conductivity of unsaturated soils.* Soil science society of America journal, 1980. **44**(5): p. 892-898.
25. Mualem, Y., *A new model for predicting the hydraulic conductivity of unsaturated porous media.* Water resources research, 1976. **12**(3): p. 513-522.
26. Schaap, M.G., F.J. Leij, and M.T. van Genuchten, *ROSETTA: a computer program for estimating soil hydraulic parameters with hierarchical pedotransfer functions.* Journal of hydrology, 2001. **251**(3): p. 163-176.
27. Leij, F.J., et al. *RETC: A computer program for analyzing soil water retention and hydraulic conductivity data*. in *Proc. Int. Workshop on Indirect methods for estimating the hydraulic properties of unsaturated soil, University of California, Riverside, CA, USA*. 1989.
28. Van Genuchten, M.T., F. Leij, and S. Yates, *The RETC code for quantifying the hydraulic functions of unsaturated soils*. 1991: Citeseer.
29. Radcliffe, D.E. and J. Šimůnek, *Soil physics with HYDRUS: modeling and applications*. 2010: CRC press Boca Raton, FL.
30. Kavetski, D., P. Binning, and S.W. Sloan, *Noniterative time stepping schemes with adaptive truncation error control for the solution of Richards equation.* Water resources research, 2002. **38**(10): p. 29-1-29-10.
31. An, H. and S. Yu, *Finite volume integrated surface-subsurface flow modeling on nonorthogonal grids.* Water Resources Research, 2014. **50**(3): p. 2312-2328.
32. Hoffmann, K.A. and S.T. Chiang, *{Computational fluid dynamics, Vol. 1}.* Wichita, KS: Engineering Education System, 2000.